

Principles of Fluorescence Correlation and Dual-Color Cross-Correlation Spectroscopy



Jan Ebenhan and Kirsten Bacia

Contents

1	Fluorescence Intensity	121
2	Fluorescence Correlation	124
3	Brightness Correlation Function	131
4	Position Correlation Function	134
	References	137

Abstract Fluorescence Correlation Spectroscopy (FCS) is a non-invasive, highly sensitive technique for measuring the diffusive and photophysical properties of fluorescent species as well as their interactions. All of this information needs to be reliably extracted from the fluctuating fluorescence signal and interpreted in a theoretical framework. In this chapter, we describe the derivation of the basic equations governing FCS correlation curves. By pointing out their limitations and the underlying approximations and assumptions we hope to facilitate applications and the development of more elaborate models for more complex systems. Two detection channels are included to accommodate dual-color Fluorescence Cross-Correlation Spectroscopy. Moreover, we provide a generalized description for the separation of spatial movement and intramolecular change, taking translational diffusion (changes in position), rotational diffusion (changes in orientation) and fluorescence blinking (changes in the quantum mechanical state) into account. Since, experimentally, particles are often labeled with multiple fluorophores, besides multiple dynamics and multiple species of particles, multiple fluorophores per particle are also part of the description.

J. Ebenhan and K. Bacia (✉)

Institute of Chemistry and Charles-Tanford-Protein-Center, Martin-Luther-Universität Halle-Wittenberg, Halle, Germany

e-mail: jan.ebenhan@chemie.uni-halle.de; kirsten.bacia@chemie.uni-halle.de

Keywords Binding analysis · Confocal microscopy · Diffusion · Fluorescence correlation spectroscopy · Fluorescence cross-correlation spectroscopy · Fluorescence spectroscopy

Fluorescence correlation spectroscopy (FCS), like dynamic light scattering (DLS), is a non-invasive and single-molecule sensitive technique based on the temporal correlation of brightness fluctuations, with which primarily the size, concentration and photophysical properties of fluorescent particles can be investigated in small liquid volumes and at thermodynamic equilibrium. It was first described in 1972 by Elliot L. Elson, Douglas Magde, and Watt W. Webb [1].

FCS is an example of a concentration correlation spectroscopy method [2]. This type of spectroscopy is based on the measurement of fluctuations of the particle concentration in small subvolumes of a sample. In principle, FCS can employ any kind of measurand that depends on these concentrations, such as density, refractive index, extinction, etc. Notably, in DLS, the signal is the amplitude of the scattered light and thus depends on the phase distribution of the electric field and the spatial variation of the permittivity in the sample. In contrast, in FCS, the intensity of the radiation constitutes the signal. Hence, the fluorescence is separated from the irradiation and the detected fluorescence photons with all their measurable properties (number, arrival time, energy, polarization, momentum direction) constitute the signal.

By virtue of the high specificity of fluorescence labeling, FCS can probe one or more defined fluorescent species even in complex mixtures and living cells and measure physical and chemical characteristics of each of them. Static and dynamic phenomena thus become accessible, provided that a detectable change in the emitted photons occurs.

For an insight into the theoretical foundations of FCS, this chapter focuses on the derivation of the underlying equations and highlights the approximations and assumptions necessary therein (Sect. 1). In many FCS applications, the translational movement of the fluorescent particles, be it diffusive or directed, can be separated from their internal changes, e.g., photophysical blinking, rotation or chemical reactions. A generalized description reflecting this property will be given to disentangle contributions from both types of processes (see Sects. 2 and 3). Furthermore, the influence of multiple species of particles (Sect. 1) as well as multiple fluorophores per particle (Sect. 2) is considered.

Multiple dynamics, multiple species and multiple fluorophores per particle are often encountered experimentally. We, therefore, aim to describe the theoretical framework in a general, adaptable way, also pointing out the limitations. Examples of calibration and control experiments, which can be conducted to check applicability, can be found in more specialized protocols, see, e.g., [3–6].

1 Fluorescence Intensity

A certain intensity of the emitted radiation of the fluorophores (in short fluorescence intensity) causes a stream of photons, which in turn is converted into a sequence of counting events in the detector. For the correlation functions considered in FCS, the stochastic properties of these events primarily produce artifacts at small correlation times, where shot noise and detector afterpulses manifest as potentially strong positive correlations. In particular, the zero value is contaminated by the variance of the Poisson distributed counting events and is not useful as a measure of the true amplitude. The considerations in this chapter therefore refer to the correlations of the fluorescence intensity itself, which are caused by molecular processes in the sample, and also no longer draw a distinction between the fluorescence intensity before the optical system and the count rate of the detector. The quantum yield of the detection Φ_D is included in the molecular brightness Q and the signal is generally denoted by F .

The molecular brightness Q of a fluorophore is generally not a constant but may depend on a number of variables, including its location \vec{r} , its orientation \vec{R} and its (quantum mechanical) state Z .

The total detected intensity can now be calculated using the so-called molecular detection function (MDF) W either as a spatial integral (with the differential volume element $d^3 \vec{r} = dx dy dz$) over the particle density C of the fluorescent particles

$$F(t) = \int W(\vec{r}, t) Q(\vec{r}, \vec{R}, Z, t) C(\vec{r}, t) d^3 \vec{r} \quad (1)$$

or as a sum

$$F(t) = \sum_i Q(\vec{r}_i, \vec{R}_i, Z_i, t) W(\vec{r}_i, t) \quad (2)$$

over the discrete contributions of individual particles i in the sample, where \vec{r}_i denotes a particle's location, \vec{R}_i its orientation and Z_i its (quantum mechanical) state.

Here, we use the discrete summation approach rather than the integral, because in this way the contributions of individual fluorophores are treated more intuitively and the probability distributions with respect to their motions and interactions are used in a more natural way. Conversely, the first approach does not require taking limits of infinite sums and it facilitates the description of spatial correlations in particles that are no longer diffusing independently as well as that of chemical reactions where the numbers and identities of particles are introduced as another random variable.

The expected value and the (cross-)correlation of the signal can now be defined starting from

$$\langle F(t) \rangle = \sum_i \langle Q(\vec{r}_i, \vec{R}_i, Z_i, t) W(\vec{r}_i, t) \rangle \quad (3a)$$

$$= \sum_i \iiint Q(\vec{r}_i, \vec{R}_i, Z_i, t) W(\vec{r}_i, t) P(\vec{r}_i, \vec{R}_i, Z_i, t) d^3 \vec{r}_i d^3 \vec{R}_i dZ_i \quad (3b)$$

$$\begin{aligned} \langle F_a(t) \cdot F_b(t + \tau) \rangle &= \sum_{ij} \int \int \int \int \int \int \\ &[Q_a(\vec{r}_i, \vec{R}_i, Z_i, t) Q_b(\vec{r}_j, \vec{R}_j, Z_j, t + \tau) \\ &P(\{\vec{r}_i, \vec{R}_i, Z_i, t\} \cap \{\vec{r}_j, \vec{R}_j, Z_j, t + \tau\}) \\ &W_a(\vec{r}_i, t) W_b(\vec{r}_j, t + \tau) d^3 \vec{r}_i d^3 \vec{r}_j d^3 \vec{R}_i d^3 \vec{R}_j dZ_i dZ_j] \end{aligned} \quad (4)$$

where the indices a and b denote different channels, each with its own molecular brightness and MDF.

The angular brackets denote an ensemble average over all possible states of the system. In the FCS experiments, this average is realized by time averaging. Throughout this chapter, ergodicity is assumed to hold. Therefore, in the limit of infinite duration of the measurement, the time average approaches the ensemble average.

The autocorrelation and cross-correlation functions are defined by $a = b$ and $a \neq b$, respectively. In the technique of dual-color fluorescence cross-correlation spectroscopy (dcFCCS) described in this chapter, the channels represent different colors, i.e. different excited and detected regions of the spectrum. However, many other possibilities are conceivable or have already been realized, e.g., spatially shifted MDFs (dual-focus FCCS [7] and multi-focus FCS [8]) or detection of different polarizations (e.g., for measuring rotational diffusion, see [9] for a detailed derivation and [10] for an application to protein oligomerization). Also related to dual-focus correlation are image correlation techniques, such as ICS, RICS, and STICS (see chapter “Theoretical Insight into the Luminescence of Dyes and Pigments” of this book), which provide spatially resolved data in, e.g., biological samples. DcFCCS has also been combined with fast camera-based imaging to generate interaction maps (see [5]).

The joint distribution $P(\{\vec{r}_i, \vec{R}_i, Z_i, t\} \cap \{\vec{r}_j, \vec{R}_j, Z_j, t + \tau\})$ indicates the probability density of finding at time t particle i at location \vec{r}_i with orientation \vec{R}_i in the (quantum mechanical) state Z_i and additionally at time $t + \tau$ particle j at location \vec{r}_j with orientation \vec{R}_j in the state Z_j . The molecular rotation contributes to the temporally correlated changes in the brightness of the fluorophore, because the orientations of the transition dipole moments of absorption and emission change relative to the electric field vector of the incident laser light and relative to the transmission direction of the polarization filter in front of the detector. The fluctuations arising from changes in the molecular orientation can be used to determine the

rotational diffusion coefficient and thus the molecular size and shape. The molecular brightness is explicitly expressed here as a function of time and location, since photophysical phenomena can lead to a variable brightness, which itself exhibits a correlation and moreover depends on location due to the spatially varying laser intensity. In most cases, Q is proportional to the product of the occupation of the excited S_1 state and the rate constant k_f of the radiative transition to the ground state. Since the degree of occupation depends on the one hand on the intensity of the excitation, but on the other hand, is also limited to unity, the brightness must always be location-dependent and must approach a limiting value of saturation for increasing excitation. The exact functional dependence on intensity can be very complicated (see [11]), but in the simplest case (laser intensity constant in time; intersystem crossing (ISC) much slower than fluorescence emission; negligible antibunching) the result is [12]

$$Q \propto \frac{k_{\text{ex}}}{1 + \frac{k_{\text{ex}}}{k_{\text{sat}}}} \quad (5)$$

where

$$k_{\text{sat}} = \frac{k_{10}}{1 + \frac{k_{\text{ISC}}}{k_{\text{phos}}}} \quad (6)$$

Here k_{ex} is the rate of excitation for the fluorophore (proportional to the exciting laser intensity I), k_{sat} is the excitation rate for which half of the maximum fluorescence brightness is obtained, k_{ISC} and k_{phos} are the rate constants of ISC and phosphorescence, respectively, and k_{10} is the rate constant for the transition to the ground state (sum of radiative and non-radiative decays).

This treatment does not account for the possibility of photobleaching and presupposes knowledge of the (often quite complex) photophysics of the fluorophores in question. For practical applications, it is therefore customary to obtain FCS measurements under a range of excitation intensities to determine the maximum usable laser power, so as to neither introduce artifacts nor unnecessarily lower the signal-to-noise ratio [13].

If several species of different brightness exist in the sample, $F(t)$ is calculated as the sum of the individual intensities according to

$$F(t) = \sum_j F_j(t) = \sum_{i,j} Q_j \left(\vec{r}_{i,j}, \vec{R}_{i,j}, Z_{i,j}, t \right) W \left(\vec{r}_{i,j}, t \right). \quad (7)$$

Here, $\vec{r}_{i,j}$ denotes the position of the i -th particle of the j -th species. $\vec{R}_{i,j}$ and $Z_{i,j}$ denote the corresponding orientations and states.

2 Fluorescence Correlation

The fundamental equation of FCS is now the normalized correlation function

$$G_{a,b}(\tau) = \frac{\langle F_a(t) \cdot F_b(t + \tau) \rangle}{\langle F_a(t) \rangle \langle F_b(t) \rangle} - 1 = \frac{\langle \delta F_a(t) \cdot \delta F_b(t + \tau) \rangle}{\langle F_a(t) \rangle \langle F_b(t) \rangle} \quad (8)$$

where $\delta F(t) = F(t) - \langle F(t) \rangle$ is the deviation of the fluorescence intensity from the expected value. Here, only positive correlation times τ are considered, because for stationary processes $G_{a,b}(-\tau) = G_{b,a}(\tau)$ applies and differences between $G_{a,b}(\tau)$ and $G_{b,a}(\tau)$ only occur in the case of a non-stationary process.

In principle, the detected radiation field depends on the exact state and motion of all molecules in the sample. Since this problem is practically unsolvable, the following assumptions and simplifications are made, unless noted otherwise:

- The MDF is time-independent: $W(\vec{r}_i, t) \mapsto W(\vec{r}_i)$.
- The polarization is uniform. This assumption is more accurate the lower the numerical aperture of the objective.
- The process can be described as weakly stationary $\langle F_a(t) \cdot F_b(t + \tau) \rangle \mapsto \langle F_a(0) \cdot F_b(\tau) \rangle$.
- The sample is stationary and isotrop ($P(\vec{r}_i, \vec{R}_i, Z_i, t) \mapsto \frac{1}{4\pi} P(\vec{r}_i, Z_i)$ with normalization $\int d^3 \vec{R}_i = 4\pi$).
- The particle density is homogeneous, implying that $P(\vec{r}_i) = \frac{1}{V}$ is the constant residence probability of the particles in the sample volume V .
- Individual fluorophores emit independently of one another, meaning there is no coherence of the fluorescence radiation and no energy transfer between the fluorophores as in FRET or fluorescence quenching.
- The particles diffuse, rotate and change their states independently of one another ($P(\{\vec{r}_i, \vec{R}_i, Z_i, t\} \cap \{\vec{r}_j, \vec{R}_j, Z_j, t + \tau\}) = P(\vec{r}_i, \vec{R}_i, Z_i, t) \cdot P(\vec{r}_j, \vec{R}_j, Z_j, t + \tau)$ for $i \neq j$).
- Rotation and diffusion do not depend on each other (absence of roto-translational coupling) and are not influenced by the state of the particle, implying that the particle does not dynamically change its shape ($P(\vec{r}_i, \vec{R}_i, Z_i, t) = P(\vec{r}_i, t) \cdot P(\vec{R}_i, t) \cdot P(Z_i, t)$).
- The translational and rotational diffusion coefficients do not depend on position or time, implying an absence of thermophoretic effects.

- Photophysical effects do not depend on spatial position ($Q(\vec{r}_i, \vec{R}_i, Z_i, t) \mapsto Q(\vec{R}_i, Z_i, t)$).
- The solvent contributes to the fluorescence only as background noise.

Thus Eq. 3b now simplifies to

$$\langle F(t) \rangle = \sum_i \iiint Q(\vec{R}_i, Z_i, t) W(\vec{r}_i) \frac{1}{4\pi V} d^3 \vec{r}_i d^3 \vec{R}_i dZ_i \quad (9a)$$

$$= \frac{\bar{Q}}{V} \sum_i \int W(\vec{r}_i) d^3 \vec{r}_i = \frac{\bar{Q}}{V} \sum_i \Omega_1 = \frac{N}{V} \bar{Q} \Omega_1 \quad (9b)$$

$$\lim_{V \rightarrow \infty} \langle F(t) \rangle = C \bar{Q} \Omega_1 = c N_A \bar{Q} \Omega_1 \quad (10)$$

Here, the brightness averaged over all orientations and possible photophysical processes is defined as

$$\bar{Q} = \iint Q(\vec{R}, Z, t) \frac{1}{4\pi} d^3 \vec{R} dZ \quad (11)$$

and the space integrals of the MDF are defined as

$$\Omega_{a,n} = \int_V [W_a(\vec{r})]^n d^3 \vec{r} \quad (12)$$

$$\Omega_{n,a;m,b} = \int_V [W_a(\vec{r})]^n [W_b(\vec{r})]^m d^3 \vec{r}. \quad (13)$$

The channel index a in $\Omega_{a,n}$ can be omitted if only one channel is used.

All identical particles contribute equally. Their contribution is proportional to their number N in the volume V . For practical purposes, the sample size can be considered as infinitely large. Under these conditions, the contribution is proportional to the particle density C or molar concentration c (where $C = N_A c$ with the Avogadro constant N_A). Finally, in the presence of several species, the total average fluorescence becomes

$$\langle F(t) \rangle = N_A \Omega_1 \sum_j c_j \bar{Q}_j \quad (14)$$

For the evaluation of Eq. 4 the double sum over the particles of the same species is split into the correlations between identical particles and the correlations between different particles. For the former, the conditional probability $P(B|A) = \frac{P(A \cap B)}{P(A)}$ is introduced. For better distinguishability of the different positions of the same

particle, the time dependence of position, orientation, and state is given in the form $x = x(0)$ and $x' = x(\tau)$:

$$\begin{aligned} & \langle F_a(0) \cdot F_b(\tau) \rangle \\ &= \sum_i \left\langle Q_a(\vec{R}_i, Z_i, 0) Q_b(\vec{R}'_i, Z'_i, \tau) W_a(\vec{r}_i) W_b(\vec{r}'_i) \right\rangle \\ &+ \sum_{i \neq j} \left\langle Q_a(\vec{R}_i, Z_i, 0) Q_b(\vec{R}_j, Z_j, \tau) W_a(\vec{r}_i) W_b(\vec{r}_j) \right\rangle \end{aligned} \quad (15a)$$

$$\begin{aligned} &= \sum_i \left\langle Q_a(\vec{R}_i, Z_i, 0) Q_b(\vec{R}'_i, Z'_i, \tau) \right\rangle \cdot \left\langle W_a(\vec{r}_i) W_b(\vec{r}'_i) \right\rangle \\ &+ \sum_{i \neq j} \left\langle Q_a(\vec{R}_i, Z_i, 0) W_a(\vec{r}_i) \right\rangle \cdot \left\langle Q_b(\vec{R}_j, Z_j, \tau) W_b(\vec{r}_j) \right\rangle \end{aligned} \quad (15b)$$

$$\begin{aligned} &= N \left[\int \int \int \int Q_a(\vec{R}, Z, 0) Q_b(\vec{R}', Z', \tau) P(\vec{R}, Z, 0) \cdot \right. \\ &P\left(\left\{ \vec{R}', Z', \tau \right\} \middle| \left\{ \vec{R}, Z, 0 \right\} \right) d^3 \vec{R} d^3 \vec{R}' dZ dZ' \left. \right] \cdot \iint W_a(\vec{r}) W_b(\vec{r}') \\ &\frac{1}{V} P\left(\left\{ \vec{r}', \tau \right\} \middle| \left\{ \vec{r}, 0 \right\} \right) d^3 \vec{r} d^3 \vec{r}' \frac{N(N-1)}{V^2} \bar{Q}_a \bar{Q}_b \Omega_{1,a} \Omega_{1,b} \end{aligned} \quad (15c)$$

$$= \bar{Q}_a \bar{Q}_b \left(\Omega_{1,a;1,b} \frac{N}{V} \Theta(\tau) \Xi(\tau) + \Omega_{1,a} \Omega_{1,b} \frac{N(N-1)}{V^2} \right) \quad (15d)$$

In Eq. 15b the averages are simplified by exploiting the presumed independence of the position and the brightness correlations (first term) and by exploiting the independence of individual particles from each other (second term). In the first term of Eq. 15c the averages are made explicit as integrals over their respective variables and the summation over identical particles is replaced by their total number N . Since one self-correlation for each particle is already contained in the first term, the sum in the second term of Eq. 15b runs over a total of $N^2 - N = N(N - 1)$ identical contributions. In Eq. 15c the second term is replaced by a term that is proportional to $N(N - 1)$ and to the product of the average intensities in both channels (see Eq. 9b). In Eq. 15d, the brightness correlation function $\Theta(\tau)$ and the position correlation function $\Xi(\tau)$ are introduced. $\Theta(\tau)$ describes the dimensionless normalized correlations of the molecular brightness $Q_{(a,b)}$ due to changes of orientation and state. $\Xi(\tau)$ describes the dimensionless normalized correlations of the apparent brightness changes due to diffusion through the focus:

$$\begin{aligned}
\Theta(\tau) &= \frac{\langle Q_a(t) \cdot Q_b(t + \tau) \rangle}{\bar{Q}_a \bar{Q}_b} \\
&= \frac{1}{\bar{Q}_a \bar{Q}_b} \int \int \int \int Q_a(\vec{R}, Z, 0) Q_b(\vec{R}', Z', \tau) P(\vec{R}, Z, 0) \\
&\quad \cdot P\left(\left\{ \vec{R}', Z', \tau \right\} \middle| \left\{ \vec{R}, Z, 0 \right\}\right) d^3 \vec{R} d^3 \vec{R}' dZ dZ' \quad (16)
\end{aligned}$$

$$\Xi(\tau) = \frac{1}{\bar{\Omega}_{1,a;1,b}} \iint W_a(\vec{r}) W_b(\vec{r}') P\left(\left\{ \vec{r}', \tau \right\} \middle| \left\{ \vec{r}, 0 \right\}\right) d^3 \vec{r} d^3 \vec{r}' \quad (17)$$

Since for infinite correlation times a complete decoupling of all fluctuations can be assumed, the conditional probability again attains the equilibrium value according to $P\left(\left\{ \vec{R}', Z', \tau \right\} \middle| \left\{ \vec{R}, Z, 0 \right\}\right) = P\left(\vec{R}', Z', 0\right) = \frac{1}{4\pi}$ and $P\left(\left\{ \vec{r}', \tau \right\} \middle| \left\{ \vec{r}, 0 \right\}\right) = P\left(\vec{r}', 0\right) = \frac{1}{V}$. The former, via Eq. 11, results in

$$\lim_{\tau \rightarrow \infty} \Theta(\tau) = 1 \quad (18)$$

and the latter in

$$\lim_{\tau \rightarrow \infty} \Xi(\tau) \propto \frac{1}{V}, \quad (19)$$

whereby an infinite sample thus leads to $\lim_{V \rightarrow \infty} \Xi(\tau) = 0$ and

$$\lim_{\tau \rightarrow \infty} \langle F_a(0) \cdot F_b(\tau) \rangle = C^2 \bar{Q}_a \bar{Q}_b \Omega_{1,a} \Omega_{1,b} \quad (20)$$

Neglecting the one particle that is correlated with itself in the second summand in Eq. 15d by approximating $N(N-1) \approx N^2$ will only be noticeable in very small compartments, for example when measuring in bacteria or lipid vesicles. After substituting these results into Eq. 8, we finally obtain

$$G_{a,b}(\tau) = \frac{\bar{Q}_a \bar{Q}_b \left(\Omega_{1,a;1,b} \frac{N}{V} \Theta(\tau) \Xi(\tau) + \Omega_{1,a} \Omega_{1,b} \frac{N(N-1)}{V^2} \right)}{\left(\frac{N}{V} \bar{Q}_a \Omega_{1,a} \right) \left(\frac{N}{V} \bar{Q}_b \Omega_{1,b} \right)} - 1 \quad (21a)$$

$$\approx \frac{\bar{Q}_a \bar{Q}_b \left(\Omega_{1,a;1,b} C \Theta(\tau) \Xi(\tau) + \Omega_{1,a} \Omega_{1,b} C^2 \right)}{(C \bar{Q}_a \Omega_{1,a}) (C \bar{Q}_b \Omega_{1,b})} - 1 \quad (21b)$$

$$= \frac{\bar{Q}_a \bar{Q}_b \Omega_{1,a;1,b} C \Theta(\tau) \Xi(\tau)}{(C \bar{Q}_a \Omega_{1,a}) (C \bar{Q}_b \Omega_{1,b})} \quad (21c)$$

$$= \frac{1}{C} \frac{\Omega_{1,a;1,b}}{\Omega_{1,a} \Omega_{1,b}} \Theta(\tau) \Xi(\tau) \quad (21d)$$

Here, the proportionality between variance and expected value of the Poisson distributed particle number in a given volume [14] becomes apparent: The numerator of the correlation function in Eq. 21c scales linearly with the concentration and quadratically with the molecular brightness. By normalizing with the square of the mean fluorescence intensity, which is proportional to the concentration squared and the molecular brightness squared, the latter no longer enters the equation, but the function as a whole increases inversely proportional with the concentration.

For practical reasons, the term $\frac{\Omega_{1,a;1,b}}{\Omega_{1,a} \Omega_{1,b}}$ is combined with the particle density and the so-called effective focal volume V_{eff} is defined as a ratio of space integrals over the MDF:

$$V_{\text{eff},x} = \frac{\Omega_{1,a} \Omega_{1,b}}{\Omega_{1,a;1,b}} \quad (22)$$

$$V_{\text{eff},(a,b)} = \frac{\Omega_{1,(a,b)}^2}{\Omega_{2,(a,b)}} \quad (23)$$

Here $V_{\text{eff},(a,b)}$ denotes the effective focal volume for the autocorrelation of one of the two channels and $V_{\text{eff},x}$ that for their cross-correlation. By introducing the effective particle number

$$N_{\text{eff}} = C V_{\text{eff}} \quad (24)$$

the general form of the F(C)CS correlation function is given by

$$G_{a,b}(\tau) = \frac{1}{N_{\text{eff}}} \Theta(\tau) \Xi(\tau) \quad (25)$$

In the case of autocorrelation, V_{eff} represents $V_{\text{eff},(a,b)}$, in the case of cross-correlation V_{eff} represents $V_{\text{eff},x}$.

The diffusion behavior of the particles has no impact on the zero value of the position correlation function $\Xi(0)$, resulting in $\lim_{\tau \rightarrow 0} \Xi(\tau) \approx 1$. Provided that the brightness is constant or correlated on significantly shorter time scales, $\lim_{\tau \rightarrow 0} \Theta(\tau) \approx 1$ also holds. Therefore, the F(C)CS amplitude is given by

$$\mathfrak{A} = \lim_{\tau \rightarrow 0} G_{a,b}(\tau) = \frac{1}{N_{\text{eff}}} \quad (26)$$

Moreover, as no motion occurs for $\tau \rightarrow 0$,

$$\lim_{\tau \rightarrow 0} P\left(\left\{\vec{r}', \tau\right\} \middle| \left\{\vec{r}, 0\right\}\right) = \delta\left(\vec{r}' - \vec{r}\right) \quad (27)$$

The double space integral thus reduces to a simple one in Eq. 17 and the origin of the normalization factor becomes apparent:

$$\lim_{\tau \rightarrow 0} \Xi(\tau) = \frac{1}{\Omega_{1,a;1,b}} \iint W_a(\vec{r}) W_b(\vec{r}') \delta(\vec{r}' - \vec{r}) d^3 \vec{r} d^3 \vec{r}' \quad (28a)$$

$$= \frac{1}{\Omega_{1,a;1,b}} \int W_a(\vec{r}) W_b(\vec{r}) d^3 \vec{r} = 1 \quad (28b)$$

Commonly, the mean fluorescence intensity from the experiment, $\langle F(t) \rangle$, is divided by the effective particle number, N_{eff} , which is readily obtained from the experimental autocorrelation curve, to yield a measure for the molecular brightness (counts per molecule, CPM), which is valid in the case of a single species. Using Eq. 10 for $\langle F(t) \rangle$ and Eqs. 22 and 24 for N_{eff} , we obtain for the counts per molecule

$$\eta = \frac{\langle F(t) \rangle}{N_{\text{eff}}} = \bar{Q} \frac{\Omega_2}{\Omega_1} \quad (29)$$

If several species of fluorophores i with their individual fluorescence intensities $F_{(a,b),i}$ and corresponding correlation functions $\Theta_i(\tau)$ and $\Xi_i(\tau)$ are present and if these fluorophores behave as independent particles in the same way as individual particles of a single species do and if no chemical reactions occur (or chemical reactions are slow compared to the time scale of the diffusion), then the following applies

$$\langle \delta F_{a,i}(t) \cdot \delta F_{b,j}(t + \tau) \rangle = \delta_{ij} \langle \delta F_{a,i}(t) \cdot \delta F_{b,i}(t + \tau) \rangle. \quad (30)$$

Equation 30 states that the fluorescence signals from different species i and j are uncorrelated. Signals are correlated if they originate from the same species ($i = j$). Since the bilinearity of the covariance leads to the additivity of the contributions of the individual species to the numerator of Eq. 8, we obtain

$$\langle F_{(a,b)}(t) \rangle = \sum_i \langle F_{(a,b),i}(t) \rangle \quad (31)$$

$$\delta F_{(a,b)}(t) = \sum_i \delta F_{(a,b),i}(t) \quad (32)$$

$$\langle \delta F_a(t) \cdot \delta F_b(t + \tau) \rangle = \sum_{i,j} \langle \delta F_{a,i}(t) \cdot \delta F_{b,j}(t + \tau) \rangle = \sum_i \langle \delta F_{a,i}(t) \cdot \delta F_{b,i}(t + \tau) \rangle \quad (33a)$$

$$= \sum_i G_{a,b,i}(\tau) \langle F_{a,i}(t) \rangle \langle F_{b,i}(t) \rangle = \sum_i \frac{1}{V_{\text{eff}} C_i} \Theta_i(\tau) \Xi_i(\tau) (\Omega_{1,a} C_i \bar{Q}_{a,i}) (\Omega_{1,b} C_i \bar{Q}_{b,i}) \quad (33b)$$

where Θ_i and Ξ_i are the brightness correlation and position correlation function for species i , respectively. In the last line Eqs. 8, 10, and 21d were used. Upon dividing by $\langle F_a(t) \rangle \langle F_b(t) \rangle$ and simplifying, the contributions of the individual species to the correlation functions can be expressed as follows, where \mathfrak{A}_i are the partial amplitudes and φ_i the amplitude fractions:

$$G_{a,b}(\tau) = \frac{\sum_i \langle \delta F_{a,i}(t) \cdot \delta F_{b,i}(t + \tau) \rangle}{\sum_i \langle F_{a,i}(t) \rangle \cdot \sum_j \langle F_{b,j}(t) \rangle} = \mathfrak{A} \sum_i \varphi_i \Theta_i(\tau) \Xi_i(\tau) \quad (34)$$

$$\mathfrak{A} = \sum_i \mathfrak{A}_i = \sum_i \frac{1}{V_{\text{eff}}} \frac{C_i \bar{Q}_{a,i} \bar{Q}_{b,i}}{\sum_j C_j \bar{Q}_{a,j} \cdot \sum_k C_k \bar{Q}_{b,k}} \quad (35)$$

$$\varphi_i = \frac{\mathfrak{A}_i}{\mathfrak{A}} = \frac{C_i \bar{Q}_{a,i} \bar{Q}_{b,i}}{\sum_j C_j \bar{Q}_{a,j} \bar{Q}_{b,j}} \quad (36)$$

The aim of the last term in Eq. 34 is to separate the different correlation functions $\Theta_i(\tau) \Xi_i(\tau)$ associated with each species from the overall amplitude \mathfrak{A} , which is oftentimes the easiest parameter to measure and interpret. The partial amplitudes \mathfrak{A}_i thus represent the (absolute) part of the amplitude belonging to species i , while the amplitude fractions φ_i represent the same value relative to the overall amplitude.

These equations are needed to analyze FCS measurements of mixtures and derive the concentrations from fitted amplitudes. It can be seen from the numerator of Eq. 35 that the amplitude fraction depends quadratically on the brightness, but linearly on the concentration of a species. This weighting causes a considerable bias toward the brighter species. If the brightnesses are not known beforehand, only apparent fractions or concentrations can be obtained and these will always underestimate the amount of dim particles in the sample.

The analysis of binding experiments relies on correlation amplitudes (see for example in [15, 16]), which can be evaluated using Eq. 35. However, to reliably determine these amplitudes, the time-dependent correlation should be analyzed by fitting Eq. 34 to the measured correlation curves. Therefore, a more detailed

examination of the brightness correlation function $\Theta(\tau)$ and the position correlation function $\Xi(\tau)$ is necessary.

3 Brightness Correlation Function

The main contributions to the time-dependent brightness fluctuations of fluorophores are given by their rotation, interaction with other particles (e.g., FRET, fluorescence quenching), chemical and photochemical reactions (e.g., cis-trans isomerization, photobleaching) and photophysical processes (e.g., ISC, antibunching). All these phenomena can be used to obtain information about molecular parameters and interactions of particles with each other (shape and size from rotation, distances from FRET, binding energies from isomerization rates, oligomerization from antibunching, etc.).

If the probability density can be completely factorized and the molecular brightness depends multiplicatively on orientation and state, then $\Theta(\tau)$ can be decomposed into a product of rotation correlation and state correlation functions. The relevant processes in FCS applications are typically transitions between states of different brightnesses of a single fluorophore, which are often described as first-order unimolecular reactions (ISC, photobleaching, antibunching). If several fluorophores (number n_F) are attached to a particle, states with several excited fluorophores exist at the same time. If the fluorophores behave independently of each other, apart from their common diffusion, the sum of their contributions can be written in analogy to Eq. 30 as:

$$Q_{(a, b)}(t) = \sum_{i=1}^{n_F} Q_{(a, b), i}(t) \quad (37)$$

$$\langle Q_a(t) \cdot Q_b(t + \tau) \rangle = \sum_{ij}^{n_F} \langle Q_{a,i}(t) \cdot Q_{b,j}(t + \tau) \rangle \quad (38a)$$

$$= \sum_{i=1}^{n_F} \langle Q_{a,i}(t) \cdot Q_{b,i}(t + \tau) \rangle + \sum_{i \neq j}^{n_F} \langle Q_{a,i}(t) \rangle \cdot \langle Q_{b,j}(t + \tau) \rangle \quad (38b)$$

$$= \sum_{i=1}^{n_F} \bar{Q}_{a,i} \bar{Q}_{b,i} \Theta_i(\tau) + \sum_{i \neq j}^{n_F} \bar{Q}_{a,i} \bar{Q}_{b,j} \quad (38c)$$

In Eq. 38c the definitions from Eqs. 11 and 16 were used. Inserting these equations back into Eq. 16 and writing

$$\bar{Q}_a \bar{Q}_b = \left(\sum_{i=1}^{n_F} \bar{Q}_{a,i} \right) \left(\sum_{j=1}^{n_F} \bar{Q}_{b,j} \right) = \sum_{i=1}^{n_F} \bar{Q}_{a,i} \bar{Q}_{b,i} + \sum_{i \neq j}^{n_F} \bar{Q}_{a,i} \bar{Q}_{b,j}, \quad (39)$$

we obtain for the total brightness correlation function

$$\Theta(\tau) = \frac{\sum_{i=1}^{n_F} \bar{Q}_{a,i} \bar{Q}_{b,i} \Theta_i(\tau) + \sum_{i \neq j}^{n_F} \bar{Q}_{a,i} \bar{Q}_{b,j}}{\sum_{i=1}^{n_F} \bar{Q}_{a,i} \bar{Q}_{b,i} + \sum_{i \neq j}^{n_F} \bar{Q}_{a,i} \bar{Q}_{b,j}}. \quad (40)$$

Subtracting one from each side and arranging yields

$$\Theta(\tau) - 1 = \sum_{i=1}^{n_F} \frac{\bar{Q}_{a,i} \bar{Q}_{b,i}}{\sum_{i=1}^{n_F} \bar{Q}_{a,i} \bar{Q}_{b,i} + \sum_{i \neq j}^{n_F} \bar{Q}_{a,i} \bar{Q}_{b,j}} [\Theta_i(\tau) - 1], \quad (41)$$

which for identical fluorophores can be simplified to

$$\Theta_{n_F}(\tau) = \frac{n_F \bar{Q}_a \bar{Q}_b \Theta_1(\tau) + n_F(n_F - 1) \bar{Q}_a \bar{Q}_b}{n_F \bar{Q}_a \bar{Q}_b + n_F(n_F - 1) \bar{Q}_a \bar{Q}_b} = \frac{\Theta_1(\tau) - 1}{n_F} + 1. \quad (42)$$

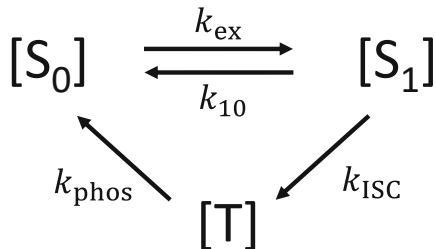
It can be seen from n_F appearing in the denominator in this last expression that a larger number of individually acting fluorophores on one particle diminishes the influence of their brightness correlation function. Since the individual brightnesses do not fluctuate in a correlated manner, the total brightness of the particle represents an average value with decreased variance.

Photophysical processes usually depend on the intensity of the exciting radiation and thus on the position of the fluorophore in relation to the focus. Therefore, not all of the assumptions made above are fulfilled and diffusion and brightness are no longer decoupled. However, a simplification can be made for slow diffusion, in which case a local photophysical equilibrium is established at any position. Although Q still depends on \vec{r} , now the relationship $\langle Q_{(a,b)}(\vec{r}_i, \vec{R}_i, Z_i, t) W_a(\vec{r}_i) \rangle = \langle Q_{(a,b)}(\vec{r}_i, \vec{R}_i, Z_i, t) \rangle \cdot \langle W_a(\vec{r}_i) \rangle$ holds. Therefore, brightness correlations and positional correlations can still be separated.

A case of practical relevance is that of the three-level system (S_0 , S_1 and T_1) with singlet-triplet transitions [17] and the rate constants k_{ex} for the excitation, k_{10} for the fluorescence and non-radiative decay, k_{ISC} for the intersystem crossing and k_{phos} for the phosphorescence.

The scheme in Fig. 1 shows the reactions which connect the populations of the three levels, $[S_0]$, $[S_1]$, $[T]$. These populations can be written as a vector, $\vec{\pi}(t)$. A corresponding system of deterministic linear differential equations with constant

Fig. 1 Scheme of the three-level system for photophysical processes used here. Arrows denote unimolecular reactions between the populations of the singlet and triplet states



coefficients can be set up to describe the kinetics and can be formulated as a matrix equation:

$$\frac{d\vec{\pi}(t)}{dt} = \mathbf{Q} \vec{\pi}(t) \quad (43)$$

This results in a 3×3 matrix for \mathbf{Q} with the rate constants given in the scheme.

$$\mathbf{Q} = \begin{pmatrix} -k_{\text{ex}} & k_{10} & k_{\text{phos}} \\ k_{\text{ex}} & -k_{10} - k_{\text{ISC}} & 0 \\ 0 & k_{\text{ISC}} & -k_{\text{phos}} \end{pmatrix}. \quad (44)$$

For the usual case $k_{10} \gg k_{\text{ISC}}, k_{\text{phos}}$, an approximate solution for the matrix equation is given by a sum of two exponential functions with characteristic time constants τ_{trip} and τ_{anti} , associated with triplet blinking and antibunching, respectively [11]:

$$\frac{1}{\tau_{\text{anti}}} = k_{\text{ex}} + k_{10} \quad (45)$$

$$\frac{1}{\tau_{\text{trip}}} = k_{\text{phos}} + \frac{k_{\text{ex}} k_{\text{ISC}}}{k_{\text{ex}} + k_{10}} \quad (46)$$

This leads to an expression for the individual correlation function $\Theta_1(\tau)$, which, by considering Eq. 42, results in [13]:

$$\Theta_{n_F}(\tau) = 1 + \frac{\bar{x}_T e^{-\tau/\tau_{\text{trip}}} - e^{-\tau/\tau_{\text{anti}}}}{n_F(1 - \bar{x}_T)} \quad (47)$$

Here, \bar{x}_T represents the average fraction of particles in the triplet state.

From this general equation many different applications can be derived, for example, the calculation of protein oligomerization via antibunching (see [18, 19]), the detection of single-nucleotide differences in DNA via their influence on blinking times (see [20]) or the study of protonation dynamics in fluorescent proteins (see [21]).

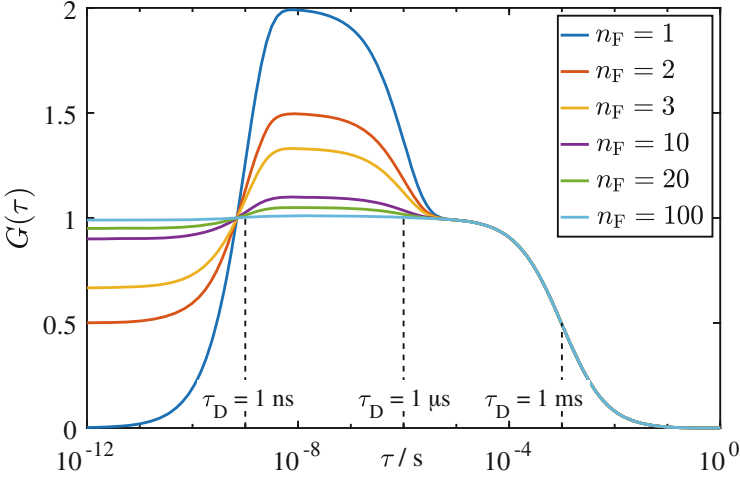


Fig. 2 Theoretical FCS correlation curves $G(\tau)$ for particles diffusing through a 3DG focus with structural parameter $S = 6$, diffusion time $\tau_D = 1$ ms and effective particle number $N_{\text{eff}} = 1$. The particles contain a varying number of fluorophores n_F given in the legend. The photophysics follows Eq. 47 with constants $\tau_{\text{anti}} = 1$ ns, $\tau_{\text{trip}} = 1$ μ s and $\bar{x}_T = 0.5$

An important result that follows from Eq. 47 is the decreasing height of the blinking term in the correlation curves with increasing number of fluorophores n_F per particle (see Fig. 2). Therefore, the blinking becomes negligible in FCS measurements of lipid vesicles with a large number of lipidic fluorophores or nanoparticles containing a large number of dyes. In this case, the blinking term does not need to be included in the fitting procedure, whereby the uncertainty in the determination of the other parameters is reduced (Fig. 2).

4 Position Correlation Function

The basis of the calculation of the position correlation function is the knowledge of the time dependence of $P(\{\vec{r}', \tau\}|\{\vec{r}, 0\})$, where the two endpoints, $\lim_{\tau \rightarrow 0} P(\{\vec{r}', \tau\}|\{\vec{r}, 0\}) = \delta(\vec{r}' - \vec{r})$ and $\lim_{\tau \rightarrow \infty} P(\{\vec{r}', \tau\}|\{\vec{r}, 0\}) = \frac{1}{V}$ are already known. In addition, for homogeneous and isotropic diffusion which is not influenced by the laser focus,

$$P(\{\vec{r}', \tau\}|\{\vec{r}, 0\}) = P(|\vec{r}' - \vec{r}|, \tau) = P(|\Delta \vec{r}|, \tau) \quad (48)$$

can be assumed, so that a function of only two parameters remains to be determined. This probability density function describes the probability of finding a particle after a certain period of time τ at a certain distance $|\Delta \vec{r}|$ from its point of origin.

Generally, diffusion models can be classified by two criteria: Fickian diffusion with a mean square deviation (MSD) of the position that increases linearly in time, and Gaussian diffusion with a normal distribution of step sizes for the particle movement, whose variance is determined by the MSD. The simplest case of free diffusion of a particle in space, without any interfering interaction with other matter, fulfills both criteria. Non-Fickian diffusion with $\langle |\Delta \vec{r}(\tau)|^2 \rangle \propto t^\nu$ is usually called anomalous diffusion [22]. Non-Gaussian yet Fickian diffusion takes place, for example, when diffusion processes with different diffusion coefficients are superimposed in complex structures [23]. Realistically, neither criterion will be fulfilled exactly, but the simple equations are used as approximations.

For isotropic Gaussian diffusion with independent motion in n spatial directions, the probability as a function of the vector $\Delta \vec{r} = (\Delta x_1, \Delta x_2, \dots, \Delta x_n)^T$ is given by [24].

$$P(|\Delta \vec{r}|, \tau) = \prod_{i=1}^n \frac{e^{-\frac{|\Delta x_i(\tau)|^2}{2\langle |\Delta x_i(\tau)|^2 \rangle}}}{\sqrt{2\pi\langle |\Delta x_i(\tau)|^2 \rangle}} \quad (49a)$$

$$= \frac{e^{-\frac{|\Delta \vec{r}|^2}{2\langle |\Delta \vec{r}(\tau)|^2 \rangle/n}}}{(2\pi\langle |\Delta \vec{r}(\tau)|^2 \rangle/n)^{n/2}}. \quad (49b)$$

If a reference measurement for $\Xi(\tau)$ is available on a system containing particles that follow Fick's law of diffusion and whose diffusion coefficient is known, a one-to-one relation between mean square displacement $\langle |\Delta \vec{r}(\tau)|^2 \rangle$ and position correlation function $\Xi(\tau)$ exists, from which first $\Xi(\tau) = f(\langle |\Delta \vec{r}(\tau)|^2 \rangle)$ and by (numerical) inversion finally $\langle |\Delta \vec{r}(\tau)|^2 \rangle = f^{-1}(\Xi(\tau))$ can be obtained. Thus, anomalous diffusion can be investigated even without explicit knowledge of $W_{(a,b)}$, which can be used e.g. for the calculation of viscoelastic properties in passive microrheology [25]. By conducting FCS measurements on different spatial scales via multiple focus sizes (spot variation FCS), the nanoscopic material properties behind the anomalous diffusion can be investigated, such as lipid domains or protein and polymer meshworks, see for example [26–28].

Nonetheless, for practical applications of the correlation functions in FCS and FCCS experiments, it is convenient to devise a model for the MDF and calculate $\Xi(\tau)$ analytically. The simplest and most common model for the MDF in a confocal setup is a three-dimensional Gaussian function (3DG) with cylindrical symmetry, where we now use the vector $\vec{r} = (x, y, z)^T$ and the center of focus is at $\vec{r} = \vec{0}$ and

the ratio of the axial vs. lateral elongation of the focus is called the structural parameter (or structure parameter) $S = \omega_z/\omega_{xy}$ [29]:

$$W_{3DG}(\vec{r}) = e^{-\frac{2(x^2+y^2)}{\omega_{xy}^2}} \cdot e^{-\frac{2z^2}{\omega_z^2}} = e^{-\frac{2(x^2+y^2+\frac{z^2}{S^2})}{\omega_{xy}^2}} \quad (50)$$

$$V_{\text{eff},x} = \left(\frac{\pi}{2}\right)^{\frac{3}{2}} \left(\omega_{xy,a}^2 + \omega_{xy,b}^2\right) \sqrt{S_a^2 \omega_{xy,a}^2 + S_b^2 \omega_{xy,b}^2} \quad (51)$$

$$V_{\text{eff},(a,b)} = \pi^{\frac{3}{2}} S_{(a,b)} \omega_{xy,(a,b)}^3 \quad (52)$$

Due to the Gaussian functions, the integration according to Eq. 17 can be solved analytically.

Introducing the diffusion time with the definition

$$\tau_{D,(a,b)} = \frac{\omega_{xy,(a,b)}^2}{4D} \quad (53)$$

as the characteristic time a particle takes to traverse the focus in lateral direction, one obtains for the position correlation function:

$$\Xi(\tau) = \left(1 + \frac{\tau}{(\tau_{D,a} + \tau_{D,b})/2}\right)^{-1} \left(1 + \frac{\tau}{(S_a^2 \tau_{D,a} + S_b^2 \tau_{D,b})/2}\right)^{-1/2} \quad (54)$$

For the experimentally important case of species of different brightnesses with a single diffusion time diffusing in 3D the FCS correlation function (not including photophysical effects) is given by [29]

$$G_{(a,b)}(\tau) = \mathfrak{A} \frac{1}{1 + \frac{\tau}{\tau_{D,(a,b)}}} \frac{1}{\sqrt{1 + \frac{\tau}{S_{(a,b)}^2 \tau_{D,(a,b)}}}} \quad (55)$$

If diffusion is restricted to a plane which is centered in the focus and perpendicular to the laser beam the MDF can be modeled as a two-dimensional Gaussian function (2DG). In this case, the FCS correlation function simplifies to

$$G_{(a,b)}(\tau) = \mathfrak{A} \frac{1}{1 + \frac{\tau}{\tau_{D,(a,b)}}} \quad (56)$$

Figure 3 illustrates the typical shapes of FCS diffusion curves for the 2DG model and for the 3DG model, including different values of the structural parameter S .

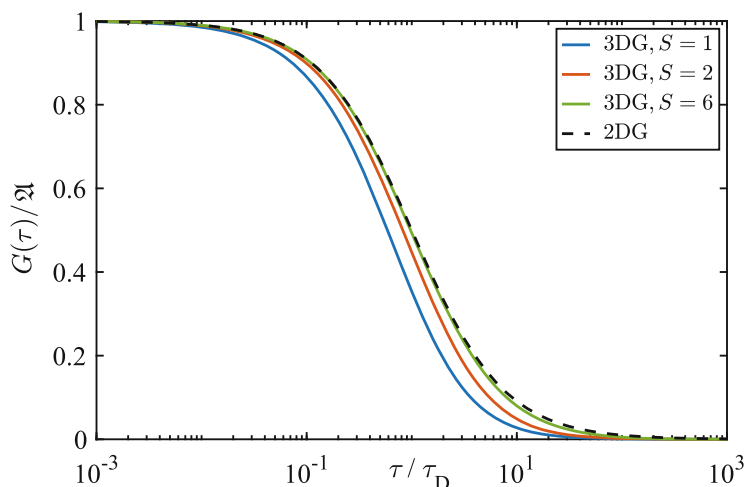


Fig. 3 Normalized theoretical FCS correlation curves, $G(\tau)/\langle I \rangle$, for a single type of diffusing particles in the absence of photophysical effects. The MDF is described by a 3DG or 2DG function for diffusion in three or two dimensions, respectively. Correlation curves for the 3DG MDF with different structural parameters S and for the corresponding two-dimensional case (2DG) are shown. For illustration purposes, the values on the abscissa are given relative to the diffusion time τ_D . For increasing values of S , the curves for the 3DG case approach their two-dimensional counterpart

References

1. Magde D, Webb WW, Elson E (1972) Thermodynamic fluctuations in a reacting system – measurement by fluorescence correlation spectroscopy. *Phys Rev Lett* 29(11):705–708
2. Elson EL, Webb WW (1975) Concentration correlation spectroscopy – new biophysical probe based on occupation number fluctuations. *Annu Rev Biophys Bioeng* 4:311–334
3. Bacia K, Haustein E, Schwille P (2014) Fluorescence correlation spectroscopy: principles and applications. *Cold Spring Harb Protoc* 2014(7):709–725
4. Bacia K, Schwille P (2007) Practical guidelines for dual-color fluorescence cross-correlation spectroscopy. *Nat Protoc* 2(11):2842–2856
5. Krieger JW, Singh AP, Bag N, Garbe CS, Saunders TE, Langowski J, Wohland T (2015) Imaging fluorescence (cross-) correlation spectroscopy in live cells and organisms. *Nat Protoc* 10(12):1948–1974
6. Malchus N (2011) Fluorescence correlation spectroscopy: detecting and interpreting the mobility of transmembrane proteins in vivo. *Curr Protoc Toxicol* 48(1):2–19
7. Dertinger T, Pacheco V, von der Hocht I, Hartmann R, Gregor I, Enderlein J (2007) Two-focus fluorescence correlation spectroscopy: a new tool for accurate and absolute diffusion measurements. *ChemPhysChem* 8(3):433–443
8. Krmpot AJ, Nikolic SN, Oasa S, Papadopoulos DK, Vitali M, Oura M, Mikuni S, Thyberg P, Tisa S, Kinjo M, Nilsson L, Terenius L, Rigler R, Vukojevic V (2019) Functional fluorescence microscopy imaging: quantitative scanning-free confocal fluorescence microscopy for the characterization of fast dynamic processes in live cells. *Anal Chem* 91(17):11129–11137
9. Loman A, Gregor I, Stutz C, Mund M, Enderlein J (2010) Measuring rotational diffusion of macromolecules by fluorescence correlation spectroscopy. *Photochem Photobiol Sci* 9(5): 627–636

10. Oura M, Yamamoto J, Ishikawa H, Mikuni S, Fukushima R, Kinjo M (2016) Polarization-dependent fluorescence correlation spectroscopy for studying structural properties of proteins in living cell. *Sci Rep* 6:1–7
11. Widengren J, Mets U, Rigler R (1995) Fluorescence correlation spectroscopy of triplet-states in solution – a theoretical and experimental-study. *J Phys Chem* 99(36):13368–13379
12. Gregor I, Patra D, Enderlein J (2005) Optical saturation in fluorescence correlation spectroscopy under continuous-wave and pulsed excitation. *ChemPhysChem* 6(1):164–170
13. Petrov EP, Schwille P (2008) State of the art and novel trends in fluorescence correlation spectroscopy. In: Resch-Genger U (ed) Standardization and quality assurance in fluorescence measurements II: bioanalytical and biomedical applications. Springer, Heidelberg, pp 145–197
14. Landau LD, Lifshitz EM (1980) Statistical physics, Part 1. Pergamon Press, Oxford
15. Jakobowska I, Becker F, Minguzzi S, Hansen K, Henke B, Epalle NH, Beitz E, Hannus S (2021) Fluorescence cross-correlation spectroscopy yields true affinity and binding kinetics of plasmodium lactate transport inhibitors. *Pharmaceuticals-Base* 14(8):757
16. Krüger D, Ebenhan J, Werner S, Bacia K (2017) Measuring protein binding to lipid vesicles by fluorescence cross-correlation spectroscopy. *Biophys J* 113(6):1311–1320
17. Bernard J, Fleury L, Talon H, Orrit M (1993) Photon bunching in the fluorescence from single molecules – a probe for intersystem crossing. *J Chem Phys* 98(2):850–859
18. Sýkora J, Kaiser K, Gregor I, Bonigk W, Schmalzing G, Enderlein J (2007) Exploring fluorescence antibunching in solution to determine the stoichiometry of molecular complexes. *Anal Chem* 79(11):4040–4049
19. Temirov J, Werner J, Goodwin P, Bradbury A (2012) “Sizing” the oligomers of Azami Green fluorescent protein with FCS and antibunching. *SPIE*
20. Yeh HC, Puleo CM, Ho YP, Bailey VJ, Lim TC, Liu K, Wang TH (2008) Tunable blinking kinetics of Cy5 for precise DNA quantification and single-nucleotide difference detection. *Biophys J* 95(2):729–737
21. Mudalige K, Habuchi S, Goodwin PM, Pai RK, De Schryver F, Cotlet M (2010) Photophysics of the red chromophore of HcRed: evidence for cis-trans isomerization and protonation-state changes. *J Phys Chem B* 114(13):4678–4685
22. Hoffing F, Franosch T (2013) Anomalous transport in the crowded world of biological cells. *Rep Prog Phys* 76(4):046602
23. Wang B, Kuo J, Bae SC, Granick S (2012) When Brownian diffusion is not Gaussian. *Nat Mater* 11(6):481–485
24. Berne B, Pecora R (1976) Dynamic light scattering. Wiley, New York
25. Rathgeber S, Beauvisage HJ, Chevreau H, Willenbacher N, Oelschlaeger C (2009) Microrheology with fluorescence correlation spectroscopy. *Langmuir* 25(11):6368–6376
26. Jin W, Simsek MF, Pralle A (2018) Quantifying spatial and temporal variations of the cell membrane ultra-structure by bimFCS. *Methods* 140:151–160
27. Šachl R, Bergstrand J, Widengren J, Hof M (2016) Fluorescence correlation spectroscopy diffusion laws in the presence of moving nanodomains. *J Phys D Appl Phys* 49(11):114002
28. Scipioni L, Lanzano L, Diaspro A, Gratton E (2018) Comprehensive correlation analysis for super-resolution dynamic fingerprinting of cellular compartments using the Zeiss Airyscan detector. *Nat Commun* 9:1–7
29. Krichevsky O, Bonnet G (2002) Fluorescence correlation spectroscopy: the technique and its applications. *Rep Prog Phys* 65(2):251–297